*Progress In Electromagnetics Research, PIER 81, 343–357, 2008*

# INVESTIGATION OF ELECTROMAGNETIC COMPLEX SCATTERING FOR CONDUCTOR TARGET BASED ON ELECTROMAGNETIC IMAGES METHOD

**Y.-L. Li**

Institute of E.M. Wave Propagation & Scattering
Xianyang Normal University
Box103, 712000, China

**J.-Y. Huang**

Science School
Xidian University
Box 273, 710071, China

**M.-J. Wang**

Institute of E.M.wave Propagation & Scattering
Xianyang Normal University
Box103, 712000, China

**Abstract**—The general image relations of electromagnetic sources are presented around a conductor sphere. The general transformations of trigonometric functions and the unit vectors between two coordinates depart from a distance are obtained. The second scattering field for a target is derived in detail. The complex scattering field and the complex RCS are gained respectively. Results show that the electromagnetic interaction of the targets must be calculated as the distance between two targets is small. The second scattering field is small to three order in magnitude to its first scattering field as the distance becomes large. The phase shift of the second field is mainly determined by the target size and the observing position and not affected greatly by its surrounding target and the distance apart. The distortion of a pulse wave is mainly induced by the phase shift of the second scattering field from the particles as the wave propagating through the random discrete medium.

# 1. INTRODUCTION

The Radar Cross Section is a very important quantity in describing the electromagnetic scattering characteristics for a target. The RCS is an essential parameter in the fields such as target detection etc., which has been studied at large by the schoolars and engineers in the world [2–18]. Before the naissance of radar, the RCS of several typical targets irradiated by a homochromous plane electromagnetic wave in free space has been presented such as a conducting sphere, a coating medium sphere, a coating cylinders and an ellipsoid. The scattering property of complex isolated targets in electromagnetic field have been also researched with the digital method and modern algorithms [19–24]. In practice, the isolated target in electromagnetic field is an ideal model, it is always electromagnetic interacting with the bodies around it. Obtaining the Complex RCS not only has the theory significance, moreover has the application value in engineering such as electromagnetic wave propagation and target identification in complex E. M. environment. Based on the literatures, this paper first presents briefly general image relation of E. M. sources around a conductor sphere, then investigates the E. M. interaction between spheres utilizing the E. M. images method. The complex RCS for the sphere is presented. Simulations of the effects induced by the target distance, target size and frequency are obtained. The results offer a support for the theoretical modeling such as target complex scattering, E. M. compatibility and multipath effect in communication channel etc.

# 2. ELECTROMAGNETIC INTERACTION BETWEEN TWO CONDUCTOR SPHERE

## 2.1. The Image Relations of Time-harmonic Electromagnetic Sources

In the time-harmonic electromagnetic field, the electric field for a point is written as

$$\mathbf{E} = -j\omega\mathbf{A} - \nabla\psi - \frac{1}{\varepsilon}\nabla \times \mathbf{A}_m$$

where $\mathbf{A}$, $\psi$, $\mathbf{A}_m$ are the vector magnetic potential, scalar electric potential and the vector electric potential respectively. They are induced respectively by the electric current, electric charge and magnetic current. As shown in Figure 1, a point electric charge $q(t)$ be put at the point depart a distance $a$ from the conductor sphere center. Its radius is $R_0$. The inductive charge on the spherical surface produces an electric field in the space which equal that produced by

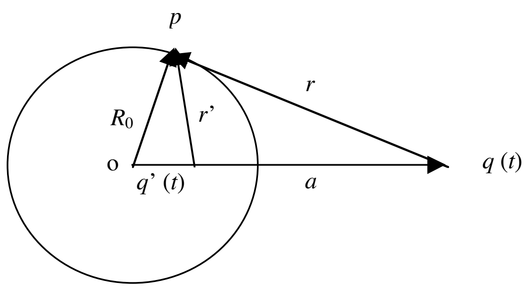


**Figure 1.** Image relation for a charge.

the image charge $q'$ inside the sphere. This image charge should locate in the line from the center to the point and depart that a distance $b$. Their retarded potentials can be written as [1]

$$\phi(r,t) = \frac{q_0 e^{j\omega t - jkr}}{4\pi\varepsilon_0 r} \quad \phi'\left(r',t\right) = \frac{q_0' e^{j\omega t - jk'r'}}{4\pi\varepsilon_0 r'}$$

Speaking to perfect conductor, the transit time is about $10^{-17}$ second [2] from a non-equilibrium state to a equilibrium state. This time correspond to the operating frequency of $10^{17}$ Hz. We thus think that the conductor surface is an equipotential plane as being irradiated by the E. M. wave, namely

$$\frac{q_0 e^{j\omega t - jkr}}{4\pi\varepsilon_0 r} + \frac{q_0' e^{j\omega t - jk'r'}}{4\pi\varepsilon_0 r'} = C$$

The followings are obtained after being the first differential to the both side to above expression

$$q_0' = -\frac{R_0}{a} q_0 \quad k' = \frac{a}{R_0} k \quad b = \frac{R_0^2}{a} \tag{1}$$

(1) states that on the case of time harmonic E. M. filed, the position of image change is same with that in static electric field, only the propagating speed has changed. On the surface of the sphere we obtain $k'r' = kr$, which ensures the potential is a constant on surface. The image relation in static electric field is the a special case of the above as $k \to 0$.

As shown in Figure 2, at the point outside the sphere, following expressions are valid both for the sources parallel to line $a$ and vertical to line $a$.

$$A_\tau = -\frac{\mu_0 I dl}{4\pi r} e^{-jkr} \cos\theta, \quad A_\tau' = -\frac{\mu_0 I' dl'}{4\pi r'} e^{-jk'r'} \cos\theta$$

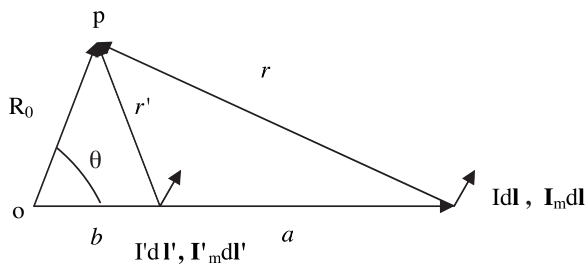


**Figure 2.** Image relation of electromagnetic sources.

Therefore, we obtain the following result using $-j\omega\left(A_\tau + A'_\tau\right) = 0$ and that in (1)

$$I'dl' = -\frac{R_0}{a} Idl \tag{2}$$

The electric field resulted by magnetic current is written as

$$\mathbf{E}_m = \frac{I_m}{4\pi}\left(\frac{1}{r} + jk\right)\frac{e^{-jkr}}{r}\hat{u}_r \times d\hat{l}, \quad \mathbf{E}'_m = \frac{I'_m}{4\pi}\left(\frac{1}{r'} + jk'\right)\frac{e^{-jk'r'}}{r'}\hat{u}_{r'} \times d\hat{l}'$$

We first express the position vectors in above with coordinates and then sum them, finally using the term that the tangential field is zero, the image relations are respectively obtained as

$$I'_m dl_\perp = -\frac{R_0}{a} I_m dl_\perp \quad I'_m dl_{//} = -\frac{R_0^3}{a^3} I_m dl_{//}$$

Generally speaking $a \gg R_0$, thus we conclude that the parallel component is higher order one and can be neglect. Therefore it is written as

$$I'_m dl_\perp = -\frac{R_0}{a} I_m dl_\perp \tag{3}$$

Expressions (1) $\sim$ (3) are the image relation. We can use them to investigate the target E. M. interaction.

### 2.2. The Scattering Field from Target 1

As shown in Figure 3, the sphere with radius $R_1$ and that with radius $R_2$ form a scattering system. The plane E. M. wave casts the system. For target 1, its scattering field has two parts, namely the first scattering field and multi-scattering. In this multi scattering field, the

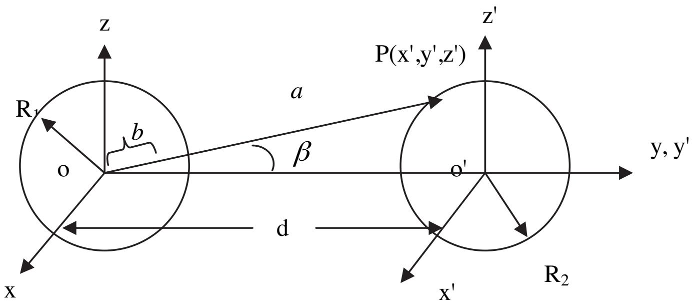


**Figure 3.** Position of two conductors.

later one's magnitude to that of the former one is $R/(8d)$. In order to briefness, we only consider the second scattering field from target 1. Symbolically [1]

$$E_{s\theta} = E_{s\theta 1} + E_{s\theta 2}, \quad E_{s\phi} = E_{s\phi 1} + E_{s\phi 2} \tag{4}$$

$$E_{s\theta 1} = f(kr)S_2(\theta)\cos\phi \tag{5}$$

$$E_{s\phi 1} = -f(kr)S_1(\theta)\sin\phi \tag{6}$$

$$E_{sr1} = j\frac{E_0\cos\phi}{k^2r^2}\sum_{n=1}^{\infty} j^{-n}a_nc_nn(n+1)\hat{H}_n^{(2)}(kr)P_n^1(\cos\theta) \tag{7}$$

$$H_{s\theta 1} = -\frac{E_{s\phi 1}}{\eta} \quad H_{s\phi 1} = \frac{E_{s\theta 1}}{\eta} \tag{8}$$

where

$$f(kr) = j\frac{E_0}{kr},$$

$$S_2(\theta) = \sum_{n=1}^{\infty} j^{-n}a_n\left[c_n\hat{H}_n^{(2)\prime}(kr)\frac{dP_n^1(\cos\theta)}{d\theta} - jd_n\hat{H}_n^{(2)}(kr)\frac{P_n^1(\cos\theta)}{\sin\theta}\right]$$

$$S_1(\theta) = \sum_{n=1}^{\infty} j^{-n}a_n\left[c_n\hat{H}_n^{(2)\prime}(kr)\frac{P_n^1(\cos\theta)}{\sin\theta} - jd_n\hat{H}_n^{(2)}(kr)\frac{dP_n^1(\cos\theta)}{d\theta}\right],$$

$$\eta = \sqrt{\frac{\mu_0}{\varepsilon_0}}$$

where $a_n$, $c_n$, $d_n$ can be seen in the literature [2], $E_{s\theta 2}$, $E_{s\phi 2}$ are respectively the second scattering field from target1 irradiating by the first scattering field from the target 2.

## 2.3. The Calculation of the Second Scattering Field

### *2.3.1. The Calculation of Electromagnetic Sources on Target 2' Surface*

If we use $\mathbf{H}_{s2}$, $\mathbf{E}_{s2}$ respectively to denote the scattering field from target 2, then the equivalent electromagnetic sources' density is written as

$$\mathbf{J}_s = \hat{r} \times \mathbf{H}_{s2}|_{r=R_2}, \quad \mathbf{J}_{ms} = \hat{r} \times \mathbf{E}_{s2}|_{r=R_2}, \quad \sigma = \varepsilon_0 \hat{r} \cdot \mathbf{E}_{s2}|_{r=R_2}$$

The exact expressions are

$$\begin{aligned} \mathbf{J}_s &= \hat{\varphi}' \frac{f(kR_2)}{\eta} S_{21} \sin\phi' - \hat{\theta}' \frac{f(kR_2)}{\eta} S_{22} \cos\phi' \\ \mathbf{J}_{ms} &= -\hat{\varphi}' f(kR_2) S_{22} \cos\phi' - \hat{\theta}' f(kR_2) S_{21} \sin\phi' \end{aligned} \tag{9}$$

$$\sigma = j \frac{\varepsilon_0 E_0 \cos\phi'}{k^2 R_2^2} \sum_{n=1}^{\infty} j^{-n} c_n (2n+1) \hat{H}_n^{(2)}(kR_2) P_n^1(\cos\theta') \tag{10}$$

$$f(kR_2) = j \frac{E_0}{kR_2},$$

$$S_{22}(\theta') = \sum_{n=1}^{\infty} j^{-n} a_n \left[ c_n \hat{H}_n^{(2)\prime}(kR_2) \frac{dP_n^1(\cos\theta')}{d\theta'} - j d_n \hat{H}_n^{(2)}(kR_2) \frac{P_n^1(\cos\theta')}{\sin\theta'} \right]$$

$$S_{21}(\theta') = \sum_{n=1}^{\infty} j^{-n} a_n \left[ c_n \hat{H}_n^{(2)\prime}(kR_2) \frac{P_n^1(\cos\theta')}{\sin\theta'} - j d_n \hat{H}_n^{(2)}(kR_2) \frac{dP_n^1(\cos\theta')}{d\theta'} \right]$$

In Figure 3, the position vector from the center of sphere 1 to the point $p$ in coordinate system $x'$-$y'$-$z'$ is expressed as

$$\mathbf{a} = \left(R_2 + d\sin\theta' \sin\phi'\right) \hat{r}' + d\cos\theta' \sin\phi' \hat{\theta}' + d\cos\phi' \hat{\phi}'$$

The distance depart from center 1 for the image is $b(R_1, R_2, \theta', \phi') = \frac{R_1^2}{|\mathbf{a}|}$. It is approximately written as

$$b\left(R_1, R_2, \theta', \phi'\right) = \frac{R_1^2}{d} \left(1 - \frac{R_2}{d} \sin\theta' \sin\phi'\right)$$

The angle formed by $b$ and $y$-axis is

$$\beta = \arcsin \frac{\sqrt{x'^2 + z'^2}}{a}$$

In general case $d \gg R_1$, $d \gg R_2$, thus we obtain

$$\beta \approx \frac{R_2}{d}, \quad b \approx \frac{R_1^2}{d}, \quad k' \approx k\frac{d}{R_1} \tag{11}$$

(11) states that we can approximately think the image locating in the line from center 1 two center 2 and the depart distance is $b$. This conclusion offers an good convenience for obtaining the radiating field induced by the images.

*2.3.2. The Calculation of the Second Scattering Field from Target 1*

The second scattering field induced by the images at $b$ has three parts, namely

$$\mathbf{E} = -\nabla\psi - j\omega\mathbf{A} - \frac{1}{\varepsilon}\nabla \times \mathbf{A}_m$$

The scalar potential resulted by the image charge is written as

$$\psi(\mathbf{r}) = \frac{1}{4\pi\varepsilon_0}\int\limits_b \frac{e^{-jk'r'}}{r'}\sigma(\mathbf{b})\,ds(\mathbf{b})$$

We put (11) into above expression and consider that $\boldsymbol{b}$ is a function of $\phi'$, $\theta'$. The integral area is on the surface at sphere 2. We put (10) into above and integral

$$\int\limits_{\pi}^{2\pi} \cos\phi' d\phi' = 0$$

It is obtained that $\psi(\mathbf{r}) = 0$, thus the electric field is zeros, namely $\boldsymbol{E}_{21} = 0$.

The vector electric potential is written as

$$\mathbf{A}(\mathbf{r}) = \int\limits_b \frac{\mu_0}{4\pi r'}e^{-jkr'}\mathbf{J}(\mathbf{b})ds(\mathbf{b})$$

By putting the first one of (9) into above and using (2) and $\int\limits_{\pi}^{2\pi} \cos\phi' d\phi' = 0$, we obtain

$$\mathbf{A}(\mathbf{r}) \approx \frac{2jE_0\mu_0 R_1 R_2 c_1 e^{-jk(r-b\sin(\theta+\beta))}}{4rdk\eta}\hat{\phi}', \quad c_1 = \int\limits_0^{\pi} S_{21}(\theta')\sin\theta' d\theta'$$

So that

$$\mathbf{E}_{22}(\mathbf{r}) \approx \frac{2E_0R_1R_2c_1e^{-jk(r-b\sin(\theta+\beta))}}{4dr}\hat{\phi}' \tag{12}$$

The unit vector $\hat{\phi}'$ is defined in sphere 2 coordinates. We must express it in sphere 1 coordinates.The following trigonometric functions are easy obtained in Figure 3.

$$\begin{gathered}\cos\theta' = \frac{r\cos\theta}{r_1'}, \quad \sin\theta' = \frac{r_2'}{r_1'} \\ \sin\phi' = \frac{r\sin\theta\sin\phi - d}{r_2'}, \quad \cos\phi' = \frac{r\sin\theta\cos\phi}{r_2'} \\ r_1' = \left(d^2 + r^2 - 2dr\sin\theta\sin\phi\right)^{\frac{1}{2}}, \quad r_2' = \left(d^2 + r^2\sin^2\theta - 2dr\sin\theta\sin\phi\right)^{\frac{1}{2}}\end{gathered} \tag{13}$$

The inverse transformation is also presented by putting $d$ into $-d$ and exchange the reciprocal quantities. The transformation between the vectors of the spherical system and that of the rectangular system are given as [2]

$$\mathbf{u} = \mathbf{Pq} \qquad \mathbf{u}' = \mathbf{P}'\mathbf{q}' \tag{14}$$

where

$$\mathbf{u} = \begin{bmatrix}\hat{u}_x \\ \hat{u}_y \\ \hat{u}_z\end{bmatrix}, \quad \mathbf{P} = \begin{bmatrix}\sin\theta\cos\phi & \cos\theta\cos\phi & -\sin\phi \\ \sin\theta\sin\phi & \sin\phi\cos\theta & \cos\phi \\ \cos\theta & -\sin\theta & 0\end{bmatrix}, \quad \mathbf{q} = \begin{bmatrix}\hat{r} \\ \hat{\theta} \\ \hat{\phi}\end{bmatrix}$$

From expression (14), we conclude that

$$\mathbf{q}' = \mathbf{P}'^{-1}\mathbf{Pq} \tag{15}$$

These expressions (13) (15) state that the unit vector of system 2 is functions of that of system 1, namely

$$\begin{gathered}\hat{\theta}' = -\frac{\left(\hat{r}f_1 + \hat{\theta}f_2 - \hat{\phi}f_3\right)r_1'r_2'}{f}, \\ \hat{\phi}' = \left[\hat{r}d\sin\theta\cos\phi + \hat{\theta}d\cos\theta\cos\phi + \hat{\phi}\left(r\sin\theta - d\sin\phi\right)\right]\frac{1}{r_2'} \\ f_1 = rd\cos\theta\sin\theta\sin\phi - d^2\cos\theta, \quad f_3 = rd\cos\theta\cos\phi\end{gathered}$$

$$f_2 = r^2 \sin\theta - 2dr \sin\phi + dr \cos^2\theta \sin\phi + d^2 \sin\theta$$

$$\begin{aligned} f \;=\; & r^4 \sin^2\theta + d^2 + 5r^2 d^2 - 4r^2 d^2 \cos^2\phi \sin^2\theta - 4d^3 r \sin\theta \sin\phi \\ & +2r^3 d \sin\theta \cos^2\theta \sin\phi - 4r^3 d \sin\theta \sin\phi \end{aligned}$$

The electric field induced by the magnetic vector potential is written as

$$\mathbf{E}_{23}(\mathbf{r}) \approx \int\limits_b \frac{1}{4\pi}\left(\frac{1}{r'} + jk\right)\frac{e^{-jkr}}{r'}\hat{r}' \times \mathbf{J}_{\perp m}(\mathbf{b}) ds(\mathbf{b})$$

By using $\int\limits_{\pi}^{2\pi} \cos\phi' d\phi' = 0$ and some calculated, we obtain the field

$$\mathbf{E}_{23}(\mathbf{r}) \approx \frac{E_0 R_2 R_1}{4\pi d^2}\frac{e^{-jk(r-b\sin(\theta+\beta))}}{r}\left(\frac{c_2 \pi d}{2}\hat{\theta}' \times \hat{r} + 2R_2 c_1 \hat{r} \times \hat{\phi}'\right) \qquad (16)$$

where $c_2 = \int\limits_0^{\pi} S_{21}(\theta') \sin^2\theta' d\theta'$.

From (12) and (16) we can obtain the second scattering field from sphere 1

$$\begin{aligned} E_{2\theta}(r) &\approx \frac{E_0 R_2 R_1}{4\pi d^2}\frac{e^{-jk(r-b\sin(\theta+\beta))}}{r} F_1, \\ E_{2\phi}(r) &\approx \frac{E_0 R_2 R_1}{4\pi d^2}\frac{e^{-jk(r-b\sin(\theta+\beta))}}{r} F_2 \\ F_1 &= \frac{2R_1 c_1 d \cos\theta \cos\phi - 2R_2 c_1 (r \sin\theta - d \sin\phi)}{r_2'} - \frac{\pi d c_2 r_1' r_2' f_3}{2f} \\ F_2 &= \frac{2R_2 c_1 d \cos\theta \cos\phi + 2R_1 c_1 (r \sin\theta - d \sin\phi)}{r_2'} - \frac{\pi d c_2 r_1' r_2' f_2}{2f} \end{aligned} \qquad (17)$$

Expression (17) is the second scattering field of sphere 1. We know that the locations both for sphere 1 and sphere 2 are symmetrical, so we can easily get the second scattering field of sphere 2 by changing the $d$ into $-d$ and mark 1 into mark 2 and mark 2 into mark 1 in above result. We conclude from (17) that the band spread and distortion effect for the pulse wave will be resulted as the wave propagating through the discrete medium. This is caused by the fact that different particle in size induces different phase shift, which is in agreement with that in the literature [7]. When $r \gg d$, the two coefficients in (17) are simplified as

$$F_1 \approx -2R_1 c_1 \quad F_2 \approx \pi d c_2 / 2$$

The above two provide a great convenience for researching the target' scattering characteristics.

### 2.4. The Effect on RCS of a Target Induced by Electromagnetic Interaction

The scattering cross section for target is defined as

$$\sigma = \frac{P}{S_i \pi a^2}$$

In which $P$ is average power scattered by a target and $a$, $S_i$ are the radius of target and incident average power density respectively. We use the expressions of (4)–(6), (17) and the orthogonality of legendre functions, namely

$$\int_{-1}^{1} P_n^m(x) P_l^m(x)\, dx = 0 \quad n \neq l$$

$$\int_{-1}^{1} P_n^m(x) P_n^l(x)\, dx = 0 \quad m \neq l$$

$$\int_0^{\pi} [P_n^1 \frac{d}{d\theta} P_{n'}^1 + P_{n'}^1 \frac{d}{d\theta} P_n^1] d\theta = 0 \quad n \neq n'$$

$$\int_0^{\pi} \left[ \frac{d}{d\theta} P_n^m \frac{d}{d\theta} P_{n'}^m + \frac{m^2}{\sin^2\theta} P_{n'}^m P_n^m \right] \sin\theta d\theta = \begin{cases} \frac{2}{2n+1} \frac{(n+m)!}{(n-m)!} n(n+1) & n = n' \\ 0 & n \neq n' \end{cases}$$

when $r \gg d$, the RCS is obtained

$$\sigma_1 = \sigma_{01} + \sigma_{i1} \tag{18}$$

where

$$\begin{aligned} \sigma_{01} &= \frac{2}{(kR_1)^2} \sum_{n=1}^{\infty} (2n+1) \left( |c_n|^2 + |d_n|^2 \right) \\ \sigma_{i1} &= \frac{R_2^2}{4\pi^2 d^4} \left( 4R_2^2 c_1 c_1^* + \frac{c_2 c_2^* \pi^2 d^2}{4} \right) + \frac{R_2}{2\pi k d R_1} \\ &\quad \iint \mathrm{Re} \left\{ j c_2 e^{-jk(b \sin(\theta+\beta))} \sum_{n=1}^{\infty} a_n \left[ c_n \frac{P_n^1}{\sin\theta} + d_n \frac{dP_n^1}{d\theta} \right] \right\} \sin\theta d\theta \end{aligned}$$

where the coefficients $c_n$, $d_n$ are defined with sphere 1. The above expression states that the second term, relative to electromagnetic interaction, is very complex and trying to obtain its analytic formula is not available. However we can get the result with computer simulation. Following parameters are used, $f = 100\,\mathrm{MHz}$, $R_1 = 1\,\mathrm{m}$, $R_2 = 2\,\mathrm{m}$ in the simulations. The wave length and target size have the same order of magnitude. The scattering effect is remarkable. The second order scattered power ratio to the first order scattered power varies with the distance of two spheres is shown in Figure 4. It implies that the second scattering power decreases greatly as the distance increasing. When $d \approx 10R_i$, the electromagnetic interaction can be neglected. As shown in Figure 5, the second scattered power does not vary greatly versus the observing point. It is determined by the targets property, target shape and the distance apart etc. and not relative to how measure the field. This interaction is about at the order of $10^{-2}$. The phase shift is gotten from (17) as

$$\psi = k\frac{R_1^2}{d}\sin\left(\theta + \frac{R_2}{d}\right)$$

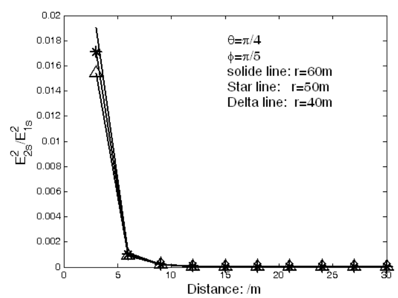


**Figure 4.** Second scattering power versus distance.

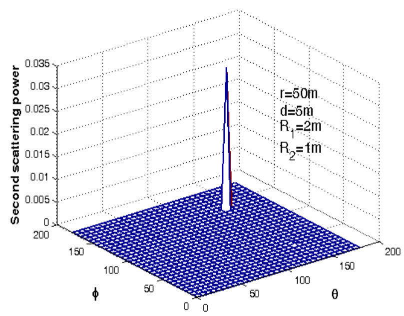


**Figure 5.** Second scattering power versus observing position.

Part simulations are shown in Figure 6 and Figure 7. It is concluded that the phase shift change sensitively with the size of target 1 and not much change with that of target 2 when the observing distance is given. When the target sizes are given, the phase shift varies with the position greatly and not much does with the distance. We so conclude that the wave distortion being measured at different point will different when a pulse wave propagating through discrete random

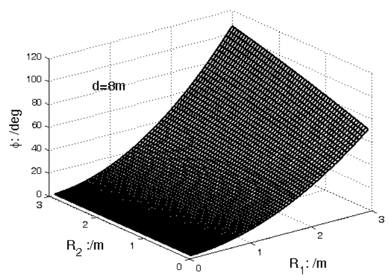


**Figure 6.** Phase shift versus target size.

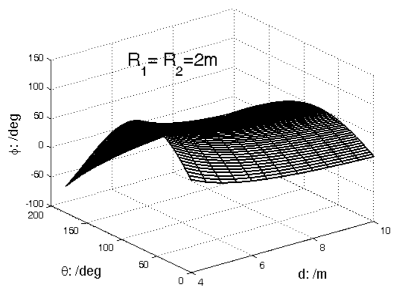


**Figure 7.** Phase shift versus azimuth and distance.

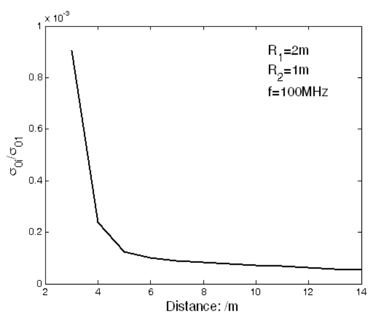


**Figure 8.** Complex RCS versus the distance.

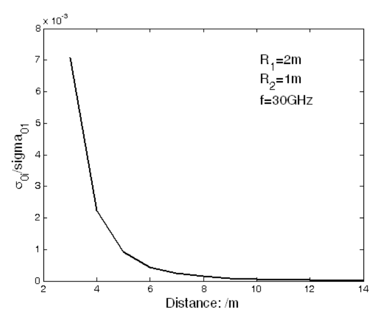


**Figure 9.** Complex RCS versus the distance.

medium. The changing of complex RCS for a target versus the distance is demonstrated in Figure 8 and Figure 9. Both in communication wave band or the $K$ wave band, the RCS induced by the electromagnetic interaction comparing with that in free space is about at the order of $10^{-3}$. This interaction will be enhanced as the operating frequency increase. Also it is concluded that the interaction can be neglected as the term $d \approx (9 - 10)R$. The results in above have a definite reference value for researching the complex polarization and complex scattering reconnaissance. More we obtain that the distortion of a wave is mainly determined by the phase shift as the wave passing the discrete medium.

## 3. CONCLUSION

The E. M. interaction between two sphere targets is researched. The image relations of E. M. sources for a conductor sphere is first presented using the boundary condition. The general transformations of trigonometric functions and the unit vectors between two coordinates depart from a distance are obtained. Based on these relations, the formula of second scattering field from a target is derived in detail. The complex RCS are thus gained. The obtained formulae are simulated. Results show that in $K$ wave band as the distance between two spheres is small, the electromagnetic interaction must be considered. When the distance $d = (8 \sim 10)R$, this interaction is neglected, the additional RCS compare with that in free space is at the order $10^{-4}$. The phase shift induced by the interaction is mainly determined by the target size and the observing point. Other objects around the target and their distance depart not effect it greatly. We so confirm that the distortion of a pulse wave is mainly induced by the phase shift of the second scattering filed from the particles as the wave propagating through the random discrete medium. The used method and the results provide a theoretical reference in the area of electromagnetic compatibility and the electric system design.

## ACKNOWLEDGMENT

The authors acknowledge the financial support of National Natural Science Foundation of China Grant Number 60741003.

## REFERENCES

1. Li, Y. and M. Wang, "The research of the image relation of electromagnetic sources around a conductor sphere," *Journal of Chongqing Institue of Technology*, Vol. 21, No. 8, 2007.
2. Wang, Y. P. and D. Z. Cheng, *Engineer Electrodynamics*, Press of Xidian University, Xian, 1985.
3. Valagiannopoulos, C. A., "Electromagnetic scattering from two eccentric metamaterial cylinders with frequency-dependent permittivities differing slightly each other," *Progress In Electromagnetics Research B*, Vol. 3, 23–34, 2008.
4. Zainud-Deen, S. H., A. Z. Botros, and M. S. Ibrahim, "Scattering from bodies coated with metamaterial using FDFD method," *Progress In Electromagnetics Research B*, Vol. 2 , 279–290, 2008.
5. Toyama, H. and K. Yasumoto, "Electromagnetic scattering from

periodic arrays of composite circular cylindrer with internal cylindrical scatterers," *Progress In Electromagnetics Research*, PIER 52, 321–333, 2005.

6. Sun, X., Y. Han, and H.-H. Wang, "Near-infrared light scattering by ice-water mixed clouds," *Progress In Electromagnetics Research*, PIER 61, 133–142, 2006.
7. Ruppin, R., "Scattering of electromagnetic radiation by a perfect electromagnetic conductor sphere," *Journal of Electromagnetic Waves and Applications*, Vol. 20, 1569–1576, 2006.
8. Hamid, A.-K., "Electromagnetic scattering from a dielectric coated conducting elliptic cylinder loading a semi-elliptic channel in a ground plane," *Journal of Electromagnetic Waves and Applications*, Vol. 19, 257–269, 2005.
9. Stratton, J. A., *Electromagnetic Theory*, McGraw-Hill, New York, 1941.
10. Huang, P. and H. Yin, *The Characteristics of Radar Target*, Publishing House of Electronics Industry, Beijing, 2005.
11. Ajose, S. O., M. N. O. Sadiku, and U. Goni, "Computation of attenuation, phase rotation, and cross-polarization of radio waves due to rainfall in tropical region," *IEEE Trans. Antennas and Propagation*, Vol. 43, No. 1, 1–5, 1995.
12. Li, Y.-L., J.-Y. Huang, M.-J. Wang, and J. Zhang, "Scattering field for the ellipsoidal targets irradiated by an electromagnetic wave with arbitrary polarizing and propagating direction," *Progress In Electromagnetics Research Letters*, Vol. 1, 221–235, 2008.
13. Censor, D., "Free-space relativistic low-frequency scattering by moving objects," *Progress In Electromagnetics Research*, PIER 72, 195–214, 2007.
14. Ishimaru, A., *Wave Propagation and Scattering in Random Medium*, Part-I, 27–30, Academic press, New York, 1978.
15. Strifors, H. C. and G. C. Gaunaurd, "Scattering of electromagnetic waves by a perfectly conducting cylinder with a thin loss magnetic coating," *IEEE Transaction on Antennas and Propagation*, Vol. 48, No. 10, 1528–1532, 2000.
16. Li, Y. and J. Huang, "The scattering fields for a spherical target irradiated by a plane electromagnetic wave in an arbitrary direction," *Chinese Physics*, Vol. 15, No. 2, 281–286, 2006.
17. Kennaugh, E. M. and D. L. Modaffatt, "Transient and impulse response approximations," *Proc. of IEEE*, Vol. 53, No. 8, 893–901, 1965.

18. Li, Y. and J. Huang, "The application of electromagnetic images method in the electromagnetic interaction between a spherical target and a conducting plane," *Journal of Electromagnetic Waves and Applications*, Vol. 21, No. 12, 1703–1715, 2007.
19. Wang, S., X. Guan, D.Wang, X. Ma, and Y. Su, "Electromagnetic scattering by mixed conducting/dielctric objects using higherorder MOM," *Progress In Electromagnetics Research*, PIER 66, 51–63, 2006.
20. Nazarchuk, Z. T. and K. Kobayashi, "Mathematical modelling of electromagnetic scattering from a thin penetrable target," *Progress In Electromagnetics Research*, PIER 55, 95–116, 2005.
21. Hongo, K. and Q. A. Naqvi, "Diffraction of electromagnetic wave by disk and circular hole in a perfectly conducting plane," *Progress In Electromagnetics Research*, PIER 68, 113–150, 2007.
22. Li, Y. and J. Huang, "The accurate solution of scattering field for a dielectric ellipsoid," *Journal of Electromagnetic Waves and Application*, Vol. 17, No. 12, 1745–1754, 2003.
23. Kotis, A. D. and J. A. Roumeliotis, "Electromagnetic scattering by a metallic spheroid using shape pertubation method," *Progress In Electromagnetics Research*, PIER 67, 113–134, 2007.
24. Lin, D. P. and H. Y. Chen, "Volume integral equation solution of extinction cross section by raindrops in the range 0.6–100 GHz," *IEEE Transaction on Antennas and Propagation*, Vol. 49, No. 3, 494–499, 2001.